The Distortion of the Cosmic Microwave Background by the Milky Way

Benjamin Czaja, Benjamin C. Bromley
University of Utah, Department of Physics and Astronomy
(Dated: July 23, 2014)

The Milky Way can act as a large-scale weak gravitational lens of the cosmic microwave background (CMB). We study this effect using a photon ray-tracing code and a Galactic mass distribution with disk, bulge and halo components. For an observer at the Sun's coordinates in the Galaxy, the bending of CMB photon paths is limited to less than one arcsecond, and only for rays that pass within a few degrees of the Galactic Center. However, the entire sky is affected, resulting in global distortions of the CMB on large angular scales. These distortions can cause the low-order multipoles of a spherical harmonic expansion of the CMB sky temperature to leak into higher-order modes. Thus the component of the CMB dipole that results from the Local Group's motion relative to the local cosmic frame of rest contributes to higher-order moments for an observer in the solar system. With our ray-tracing code we show that the phenomenon is not sensitive to the specific choice of Galactic potential. We also quantitatively rule it out as a contributor to CMB anomalies such as power asymmetry or correlated alignment of low-order multipole moments.

PACS numbers:

arXiv:1407.5686v1 [astro-ph.CO] 21 Jul 2014

INTRODUCTION

As an echo of the hot big bang, fluctuations in the cosmic microwave background are snapshots of seeds of cosmic structure, including galaxies, galaxy clusters and the large-scale network of voids, filaments, and superclusters. NASA's *Cosmic Background Explorer* first detected these fluctuations, which appear as angular anisotropies on the plane of the sky [1]. More recently the *Wilkinson Microwave Anisotropy Probe* [2] and the *Planck Collaboration* [3] have mapped out these temperature fluctuations in exquisite detail, allowing for precise assessment of cosmological parameters such as the global mass density and the baryon fraction [4].

Distortions of the cosmic microwave background by sources between the surface of last scattering and an observer in the present day can measurably alter the primordial CMB. For example, the Sachs-Wolf effect of gravitational red shifting that results from evolving large-scale structure can generate anisotropies in the CMB sky temperature [5]. Additional anisotropies arise from the Sunyaev-Zeldovich effect of photon scattering by hot gas in galaxy clusters [6]. Weak gravitational lensing by smaller-scale structures, including individual distant galaxies, can produce fluctuations as well. [for a review, see 7].

The CMB also exhibits temperature anisotropies on the largest scales. In addition to the Doppler affect that produces the dominant dipole feature [8], the CMB has quadrupole and octupole modes that may be aligned as compared with a statistically isotropic field [9]. Furthermore, the statistics of temperature fluctuations within separate hemispheres of the sky are significantly different, yielding asymmetric power spectra [10–12]. These large-scale anomalies challenge a fundamental assumption of modern cosmology, that the universe is statistically isotropic and homogeneous.

Here we focus on gravitational lensing of the CMB by the largest structure in the sky, our own Galaxy. This effect will be weak: Indeed if the CMB were perfectly isotropic, and if the Galaxy and observers within it were at rest in the CMB's reference frame, then lensing would produce no temperature anisotropies. However, the Galaxy is moving with respect to the CMB, and observers in the Galactic rest frame see anisotropies from the relativistic Doppler shift of CMB photons. In terms of spherical harmonic expansions of the CMB temperature maps, the dipole is most prominent, with weak contributions from higher-order modes [13]. It is this Doppler shifted map that Galactic lensing distorts. Since the dipole is strong, the distortions might generate higher-order multipoles at measurable levels.

In this paper, we select models of the Galaxy's mass distribution and present a ray-tracing algorithm to track photon trajectories in these models (§2). We then consider how a uniform CMB signal is affected by the motion of the Galaxy relative the CMB's frame of reference, and the Galactic potential (§3). We show that lensing mixes the dipole signal with higher-order spherical harmonic modes of the CMB fluctuations in the plane of the sky. Finally we discuss our results in the context of experimental measurements of the CMB.

WEAK LENSING BY THE GALAXY

Ray Tracing through the Milky Way

To map photon trajectories through a gravitational potential Φ, we start at the observer location near the Sun, taken to be 8.0 kpc from the Galactic Center in the plane of the disk. We ray-trace back in time, using initial velocities aimed at points on a regular grid of Galactic latitude

and longitude coordinates in the observer's sky. A 4-th order Richardson extrapolation integrator [14] solves the spatial part of the photon geodesic equation in the limit of a weak, static source of gravity,

$$\ddot{\vec{x}} = -2\vec{\nabla}_\perp \Phi, \tag{1}$$

where the spatial derivative is the component of the gradient that is perpendicular to the photon velocity. Integration ends when a photon has reached a distance of several hundred kpc or more from the Galactic Center.

We select the gravitational potential Φ from a suite of published models: Kenyon et al. [15], Paczynski [16], Johnston et al. [17], Dauphole & Colin [18], and Allen & Santillan [19]. These models all contain disk (Miyamoto-Nagai [20]), bulge (Hernquist [21], Plummer [22]), and halo components (Navarro-Frenk-White [23]). Where the mass is divergent, we take the extent of the models to be 300 kpc. Our results are not sensitive to this choice, or to the radial limit of photon integration. While we do find some sensitivity to specific models, our overall conclusions hold for all models. Unless otherwise specified, we adopt the form of Φ from Kenyon et al. [15].

Temperature maps and spherical harmonic coefficients

To create a map of sky brightness, we sample the full grid of angular coordinates, with $N_b \times N_\ell$ points in latitude b and longitude ℓ. A "pixel" with index ij has sky location (b_i, ℓ_j) with $0 \le i < N_b$ and $0 \le j < N_\ell$; the unit vector $\hat{n}_{ij}$ aimed out from the observer in that direction gives the initial direction of the photon ray associated with that pixel. Lensing can change the final direction of that ray, given by $\hat{n}'_{ij}$; a deflection angle

$$\Psi_{ij} = \arccos(\hat{n}'_{ij} \cdot \hat{n}_{ij}) \tag{2}$$

provides a measure of the lensing effect. Fig. 1 provides an illustration, showing deflection angles as a function of sky position. In this case, the maximum deflection angle is limited to approximately one arcsecond.

The sky brightness measured at a pixel in direction $\hat{n}$ depends on the brightness of the primordial CMB in direction $\hat{n}'$. Modifications to this primordial signal include a Doppler shift from the peculiar motion of the Galaxy, a gravitational redshift from the Galactic potential, and a cosmological redshift. A single factor g, the ratio of an observed photon's frequency ν relative to its frequency ν' at the surface of last scattering, can account for both the cosmological and gravitational redshifts. We do not attempt to disentangle them — the cosmological redshift will be overwhelmingly dominant — because they do not affect the anisotropy of sky temperature. Since the CMB's specific intensity I_ν corresponds to a Planck function $B_\nu(T)$ at temperature T, and since I_ν/ν^3 is a Lorentz invariant (conservation of photon number along a ray), it follows that

$$I_\nu(T) = B_\nu(T) = B_\nu(gT_s), \tag{3}$$

where T_s is the CMB temperature at the surface of last scattering.

Compared to the redshift of CMB photons, the Doppler effect of the Galaxy plowing through the CMB is more complicated. We view it as the result of a boost from the frame of the CMB to the frame of the Galaxy, in which we calculate the gravitational lensing. For definiteness, we assume that the velocity of the Galaxy relative to the CMB, $\vec{V}$, has a magnitude of 627 km/s and direction $(\ell, b) = (30°, 276°)$, corresponding to the Local Group [24]. Taking into account the lensing of the CMB, the observed blackbody temperature in a specific direction $\hat{n}$ is

$$T(\hat{n}) = \frac{gT_s\sqrt{1 - V^2/c^2}}{1 - \hat{n}' \cdot \vec{V}/c} \tag{4}$$

$$\approx gT_s\left[1 + \frac{V}{c}\cos\theta + \frac{V^2}{2c^2}\cos 2\theta + \mathcal{O}\left(\frac{V^3}{c^3}\right)\right] \tag{5}$$

where θ is the angle between $\hat{n}'$ and $\vec{V}$. With the ray-tracer to calculate $\hat{n}'$, we find $T(\hat{n})$ for each pixel and build up a temperature map for any Galactic potential, covering the full sky with up to 10^8 pixels.

To measure the impact of lensing on the CMB, we work with conventional spherical harmonic expansion coefficients,

$$a_{\ell,m} = \int_0^{2\pi}\int_0^{\pi} T(\hat{n}) Y^*_{\ell,m}(\theta,\phi)\sin(\theta)\, d\theta d\phi \tag{6}$$

where the sky temperature T is measured along a lensed ray. We estimate these coefficients—and their values in the limit of no lensing—from the pixel maps using a third-order accurate Newton-Cotes integration scheme. Our results below are reported in terms of C_ℓ, defined as the absolute square of the expansion coefficients for a particular ℓ, averaged over m values.

RESULTS

In principle the lensing of light rays over the sky maps out the gravitational potential of the Milky Way. Since the sun is not located at the center of the Galaxy we observe a distinct lensing pattern, as in Fig. 1. The strongest lensing is in the direction of the bulge of the Milky Way, a region where stars are densely clustered. However lensing still occurs across most of the sky as a result of the dark matter halo. When the Galaxy is moving with respect to the CMB rest frame, the resulting dipole becomes a "background" signal that can leak into other CMB modes as a result of the combination of the

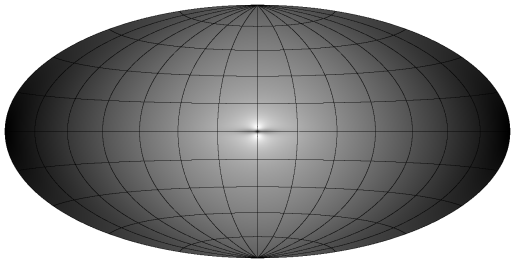

FIG. 1: An Aitoff projection of lensed light rays by the Milky Way forming a pattern across the entire sky. The area on the sky where the light rays were lensed the most appears lighter, where the light rays were lensed the least the appears darker. The maximum deflection angle is approximately $0.8''$

sun's location away from the Galactic Center and the small-magnitude but large-scale deflection of light rays.

Fig. 2 compares the Doppler effect both with and without lensing. The two cases have similar mode amplitudes up to the octupole terms, however, higher-order modes show remarkable differences. The fall-off in the lensed CMB spectrum is slow but steady with increasing ℓ, while the Doppler effect on its own plummets, as expected from Eq. 5. Table I gives a more quantitative comparison of the low-ℓ angular power spectrum in terms of the amplitude spectral density, $\propto \sqrt{C_\ell}$.

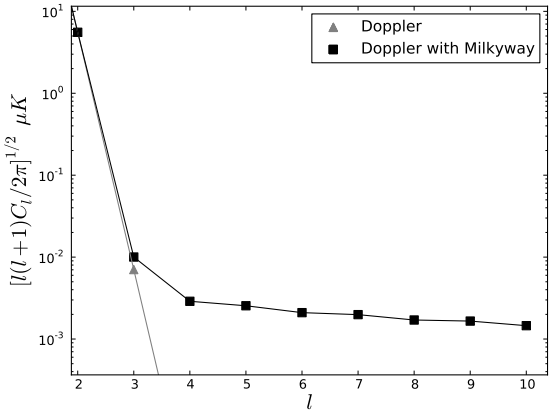

FIG. 2: Amplitude of spherically-averaged large-angle anisotropies due to the Doppler effect from the motion of our Galaxy (triangles), and further including the effect of gravitational lensing by the Galaxy (squares), as a function of angular scale (given in terms of multipole index ℓ). For the octupole and higher-order terms, the distortions from lensing dominate the Doppler effect.

Fig. 3 demonstrates the sensitivity of the lensing effect to the model of the Galactic potential. The overall power spectrum is similar in all cases. Differences between the models, while small, illustrate that the Milky Way lensing effect may provide some level of discrimination between them, at least in the idealized setting afforded by our ray-tracing experiments. Even if models of the Galaxy are not distinguishable, broader properties of the Galaxy might be assessed. For example the strength of the low-ℓ modes scale with Galactic mass, M, assuming that the radial extent of the Galaxy is fixed. Then the spectrum of mode amplitudes for $\ell \geq 4$ will depend on mass ,scaling roughly as $10^{-8}/\ell \times M/(10^{10}\ M_\odot)$.

We also determine the effect of a sky mask that excludes regions near the Galaxy's disk plane where gas and dust can contaminate the CMB signal. Specifically

TABLE I: The temperature anisotropies induced by the Doppler effect from the Galaxy's motion, with and without a contribution from lensing, on large angular scales. The first column is the multipole index, while the angle-averaged mode amplitudes for a Doppler only model (no lensing), and the Doppler effect along with lensing are in the middle and right columns, respectively.

mode	amplitude ($[l(l+1)C_l/2\pi]^{1/2}K$)	
ℓ	Doppler only	Doppler with lensing
1	$3.83 \cdot 10^{-3}$	$3.83 \cdot 10^{-3}$
2	$5.55 \cdot 10^{-6}$	$5.55 \cdot 10^{-6}$
3	$7.04 \cdot 10^{-9}$	$9.52 \cdot 10^{-9}$
4	$<10^{-12}$	$2.49 \cdot 10^{-9}$
5	$<10^{-12}$	$2.14 \cdot 10^{-9}$
6	$<10^{-12}$	$1.81 \cdot 10^{-9}$
7	$<10^{-12}$	$1.67 \cdot 10^{-9}$
8	$<10^{-12}$	$1.48 \cdot 10^{-9}$
9	$<10^{-12}$	$1.40 \cdot 10^{-9}$
10	$<10^{-12}$	$1.27 \cdot 10^{-9}$

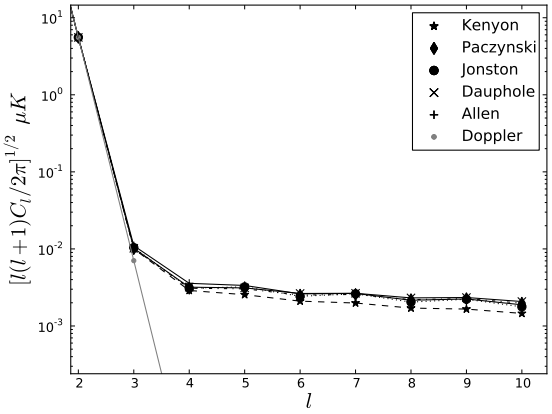

FIG. 3: The amplitude spectrum of fluctuations that results from the Doppler effect and gravitational lensing as predicted in a set of Galactic potential models. The models are labeled Kenyon (stars), Paczynski (diamonds), Jonston (black circles), Dauphole (x), and Allen (crosses), as described in the text. For comparison, the Doppler-only model (grey circles) is also shown falling off abruptly with angular scale. The Galactic mass models all give results that are similar to one another and all generally overwhelm the Doppler-only spectrum at $\ell > 3$.

we mask out low Galactic latitudes $|b| \leq 10^\circ$, setting the sky temperature to zero in the masked region. In this way we get a general idea of how a Galactic cut may affect the strength of the lensed CMB. Table II shows the difference in spectral amplitude ($\propto$ the square root of the power, as in Table I) between the lensed and unlensed cases in the presence of the mask. We see that the effect of the cut generates a signal at a level of $10^{-4}\mu K$ for low $\ell > 3$, an order of magnitude below the unmasked signal. This reduction is mitigated somewhat if we estimate the power from the cut-sky map by renormalizing to the fraction of the sky that is retained in the map.

TABLE II: The contribution to the amplitude spectrum by gravitational lensing when a low-latitude Galactic cut is applied. The first column is the multipole index, while the second column is the difference between the multipole amplitude with and without lensing. Here, all amplitudes are measured after we mask the low-latitude region by setting the sky temperature to zero wherever $|b| \leq 10^\circ$.

mode ℓ	amplitude difference $[\ell(\ell+1)C_\ell/2\pi]^{1/2}K$
1	$8.59 \cdot 10^{-10}$
2	$1.70 \cdot 10^{-10}$
3	$2.31 \cdot 10^{-10}$
4	$1.34 \cdot 10^{-10}$
5	$5.10 \cdot 10^{-10}$
6	$1.28 \cdot 10^{-10}$
7	$5.34 \cdot 10^{-10}$
8	$1.11 \cdot 10^{-10}$
9	$4.90 \cdot 10^{-10}$
10	$8.60 \cdot 10^{-11}$

DISCUSSION

Here we calculate the deflection of cosmic photons by the gravity of the Milky Way. All-sky deflection maps show how a background reference signal might be distorted, although the angles involved are small (less than an arcsecond). Nonetheless, if some such background exists, as in the case of of distant galaxies in the study of cosmological weak lensing, then the Milky Way's full gravitational potential could be revealed.

We illustrate this effect with the CMB temperature. The dipole signal from the Galaxy's motion through the CMB serves as a reference signal, and distortions from gravitational lensing are measured in terms of leakage into quadrupole and higher-order modes. We demonstrate that the effect is orders of magnitude too small to account for anomalies like the hemisphere power asymmetry or quadrupole-octupole alignment. Indeed, the cosmological signal in the CMB sky temperature overwhelms the lensing effect described here. However, as technology improves, power from lensing might contribute at a measurable level.

Even with existing data, we can use the lensing effect reported here to place very crude astrophysical constraints. Galaxy potential models in which the mass normalization is a parameter give a limit of $\sim 10^{15}$ $M_\odot$ for the total mass to the Milky Way. While not useful in terms of understanding our own Galaxy, this exercise reflects the well-known idea that CMB lensing can yield mass estimates for distant galaxy clusters [25–27]. Our ray-tracing code suggests that the lensing effect may help place limits on nearby objects as well. Perhaps Andromeda or the Virgo cluster might offer opportunities closer to home.

We thank an anonymous referee for suggestions that improved the focus and presentation of the manuscript. We are grateful to the University of Utah for support through the Undergraduate Research Opportunities Program and to NASA for a generous allotment of computer time on the discover cluster.

[1] Smoot, G. F., Bennett, C. L., Kogut, A., et al. 1992, Astrophys. J. , 396, L1
[2] Bennett, C. L., Larson, D., Weiland, J. L., et al. 2013, ApJS, 208, 20
[3] Planck Collaboration, Ade, P. A. R., Aghanim, N., et al. 2013, arXiv:1303.5062
[4] Tegmark, M., Strauss, M. A., Blanton, M. R., et al. 2004, Phys. Rev. D , 69, 103501
[5] Sachs, R. K., & Wolfe, A. M. 1967, Astrophys. J. , 147, 73
[6] Sunyaev, R. A., & Zeldovich, Y. B. 1972, Comments on Astrophysics and Space Physics, 4, 173
[7] Lewis, A., & Challinor, A. 2006, Phys. Rep., 429, 1
[8] Lineweaver, C. H., Tenorio, L., Smoot, G. F., et al. 1996, Astrophys. J. , 470, 38
[9] Tegmark, M., de Oliveira-Costa, A., & Hamilton, A. J. 2003, Phys. Rev. D , 68, 123523
[10] Eriksen, H. K., Hansen, F. K., Banday, A. J., Górski, K. M., & Lilje, P. B. 2004, Astrophys. J. , 605, 14
[11] Hansen, F. K., Banday, A. J., & Górski, K. M. 2004, Mon. Not. R. Astron. Soc,, 354, 641
[12] Planck Collaboration, Ade, P. A. R., Aghanim, N., et al. 2013, arXiv:1303.5083
[13] Kamionkowski, M., & Knox, L. 2003, Phys. Rev. D , 67, 063001
[14] Bromley, B. C., & Kenyon, S. J. 2006, AJ, 131, 2737
[15] Kenyon, S. J., Bromley, B. C., Geller, M. J., & Brown, W. R. 2008, Astrophys. J. , 680, 312
[16] Paczynski, B. 1990, Astrophys. J. , 348, 485
[17] Johnston, K. V., Spergel, D. N., & Hernquist, L. 1995, Astrophys. J. , 451, 598
[18] Dauphole, B., & Colin, J. 1995, A&A, 300, 117
[19] Allen, C., & Santillan, A. 1991, Rev. Mexicana Astron. Astrofis., 22, 255
[20] Miyamoto, M., & Nagai, R. 1975, Publ. Astron. Soc. Jpn., 27, 533
[21] Hernquist, L. 1990, Astrophys. J. , 356, 359
[22] Plummer, H. C. 1911, Mon. Not. R. Astron. Soc,, 71, 460
[23] Navarro, J. F., Frenk, C. S., & White, S. D. M. 1997,

Astrophys. J. , 490, 493
[24] Kogut, A., Lineweaver, C., Smoot, G. F., et al. 1993, Astrophys. J. , 419, 1
[25] Seljak, U., & Zaldarriaga, M. 2000, Astrophys. J. , 538, 57
[26] Vale, C., Amblard, A., & White, M. 2004, New Astronomy, 10, 1
[27] Yoo, J., & Zaldarriaga, M. 2008, Phys. Rev. D , 78, 083002